

Microstructure and mechanical properties of polycrystalline NbN/TaN superlattice films

JUNHUA XU, MINGYUAN GU, GEYANG LI

State Key Laboratory of MMCs, Shanghai Jiao-Tong University, Shanghai 200030, People's Republic of China

E-mail: sklmmc@mail.sjtu.edu.cn

The polycrystalline NbN/TaN superlattice films have been grown on the substrates of 18-8 stainless steel by reactive magnetron sputtering. The microstructure and microhardness of the superlattice films have been studied with X-ray diffraction (XRD), high resolution transmission electron microscopy (HREM) and microhardness tester. The results showed that the NbN layers are of face cubic and the TaN layers are hexagonal crystal structure in the NbN/TaN superlattice films. The lattice plane (111) of NbN are coherent with the (110) of TaN and the lattice mismatch is 3.18%. The NbN/TaN superlattice film demonstrated superhardness effects. The maximum Knoop hardness value reached 5100 kgf/mm² with a modulation period from 2.3 nm to 17.0 nm. It was proved that even if NbN layers did not take the same crystal structure as TaN layers, hardness anomalous phenomenon still can be produced as long as the coherent strains exist. © 2000 Kluwer Academic Publishers

1. Introduction

TiN films deposited by physical vapor deposition (CVD) method have found widespread application in wear resistant situation such as cutting tools or mechanical parts because of its high hardness, wear resistance, chemical inertness and high temperature stability. However, the hardness of the TiN coatings (<2500 kgf/mm²) are not high enough for some applications, and there is thus a driving force to find new coatings suitable for such applications. Recently very large modulus or hardness increases have been reported in some multilayer thin films [1–5]. It is called “supermodulus” or “superhardness” effect, which has received the most attention.

Helmerson *et al.* [1] first investigated the change rule of microhardness vs. modulation period (Λ) in the strained coatings of TiN/VN single-crystal superlattice. The results showed that the microhardness of the TiN/VN were 2.5 times higher than that of the alloy Ti_{0.5}V_{0.5}N films. Mirkarimi, Chu *et al.* [2–4] have studied the relationships between the microhardness and the modulation period of single-crystal superlattice TiN/NbN and TiN/V_{0.6}Nb_{0.4}N, polycrystalline superlattice TiN/NbN and TiN/VN multilayer films. The microhardness anomalies were found in these systems. Several theories were proposed in the literatures to explain the mechanisms of hardness anomalies. They are: (1) dislocation generation and mobility mechanisms according to Hall-Petch formula. (2) supermodulus effect model, hardness anomalies resulted from modulus anomalies caused by Fermi surface-Brillouin zone interaction or interfacial coherent strain. (3) grain refinement theory, the grain size tends to be limited by the layer thickness. In fact, each hardening theory pro-

posed so far could only explain some phenomena of the researched systems, but not suitable for every system.

In the ceramic multilayer system, the mechanical properties of the epitaxial growth films with the same crystal structure have been reported. It is well known that NbN and TaN have two crystal structures: face cubic and hexagonal. The lattice constants of the face cubic structure of TiN and TaN are 0.439 nm and 0.440 nm respectively whose lattice mismatch is only 0.2%. But the hexagonal lattice parameters of NbN and TaN are $a = 0.2968$ nm, $c = 0.5548$ nm and $a = 0.5192$ nm, $c = 0.2908$ nm respectively, which have a very large difference. In the paper, NbN/TaN nanomultilayers have been synthesized. The aim is to investigate the growth model of the interfaces and the mechanical properties of the NbN/TaN multilayer thin films.

2. Experimental procedure

The polycrystalline NbN/TaN ceramic nano-multilayer films were deposited using SPC-350 magnetron sputtering system, which has three targets including one d.c. magnetron cathode and two r.f. magnetron cathodes. Sputtering targets were pure Nb (99.9%) and Ta (99.9%) which were mounted on the d.c. and r.f. cathodes, respectively. After base pressures of 1×10^{-4} Pa was obtained, Ar and N₂ were bled into the chamber through two separate gas manifolds. A mixed Ar-N₂ gas was used for reactive sputtering with an Ar partial pressure of 3.4×10^{-1} Pa and a N₂ partial pressure of 0.4×10^{-1} Pa. Ground and polished stainless steel wafers were used as deposition substrates. They were ultrasonically cleaned in chemical solvents before being mounted onto the substrate holder in

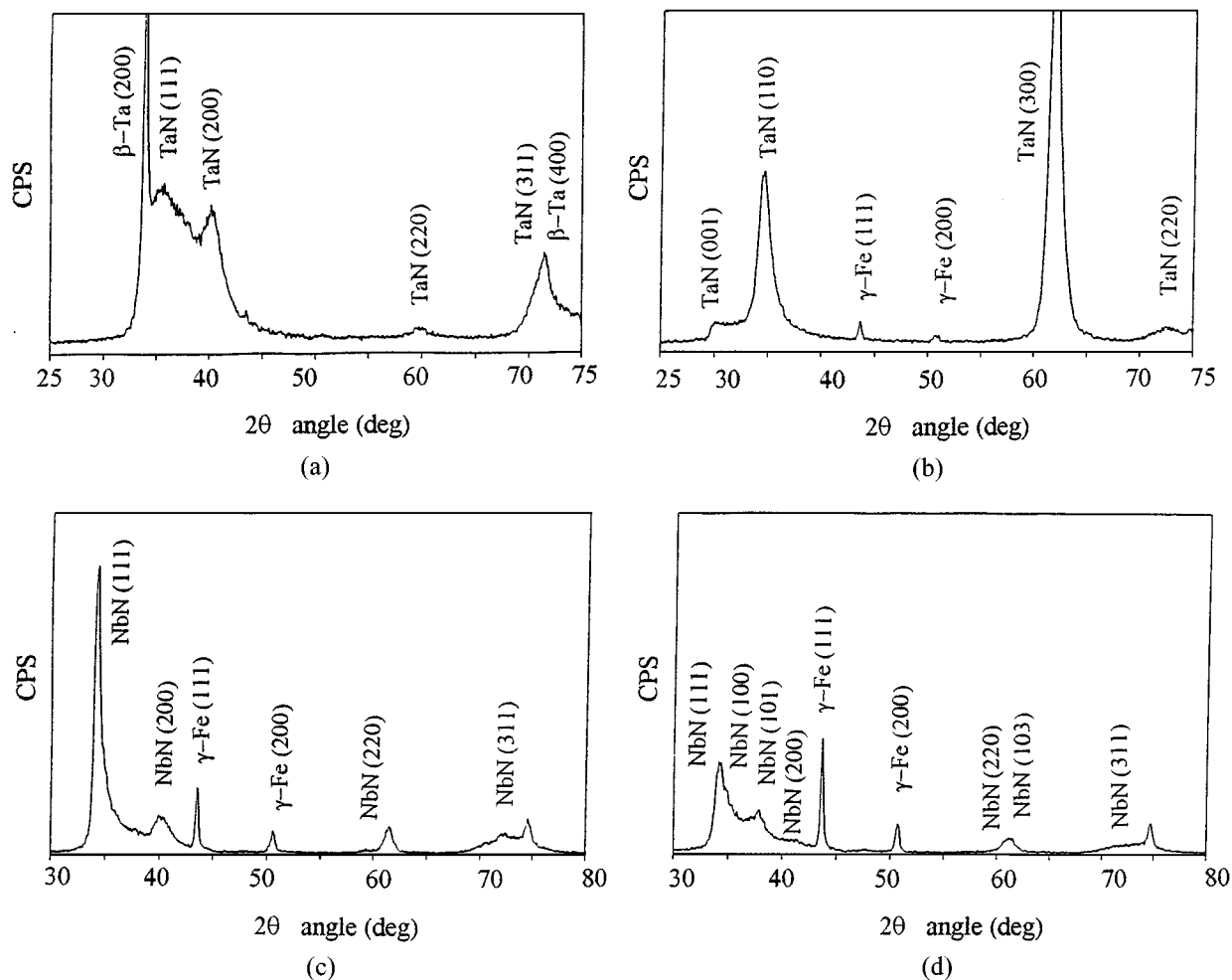


Figure 1 XRD spectra of single-layer films. (a) TaN, $P_{N_2} = 0.2 \times 10^{-1}$; (b) TaN, $P_{N_2} = 0.4 \times 10^{-1}$; (c) NbN, $P_{N_2} = 0.2 \times 10^{-1}$; (d) NbN, $P_{N_2} = 0.4 \times 10^{-1}$.

the chamber. Modulation structures were obtained by rotating the substrate holder, letting samples to face Nb and Ta targets. The designed modulation ratio was $l_{TaN}/l_{NbN} = 1 : 1$. Modulation ratios were obtained through exact control of the stopping time in front of the Nb and Ta targets. In order to improve the adhesion between the film and the substrate, a titanium underlayer of 150–200 nm was first deposited on the substrate and then alternately deposited the NbN and the TaN layers. The source power of Ta and Nb targets were 100 W and 0.15 A \times 400 V respectively. The deposition rate was 0.32 nm/sec for TaN and 0.30 nm/sec for NbN. The total thickness of multilayer films were 2.0 μ m. The substrates were heated to 400°C before deposition and the deposition temperature was below 70°C.

The hardness of multilayer films was measured using a MHT-1 microhardness tester. A Knoop diamond tip indenter was used at a load of 25 gf for 15 seconds. This indent geometry was chosen because of its large ratio of the diagonal length to the depth which can decrease the effect of substrate hardness on the hardness of films. Ten indentations were made at each load. The crystal structure of multilayer films was determined by X-ray diffraction (XRD) in a D/max-3A diffractometer with Cu K_{α} radiation. The JEM-200CX transmission electron microscope was used to study cross-sectional microstructure of samples.

3. Experimental results

3.1. X-ray diffraction

X-ray diffraction spectra of single layer NbN and TaN films under the deposition condition of $P_{N_2} = 0.2$ – 0.4×10^{-1} Pa, $P_{Ar_2} = 3.4 \times 10^{-1}$ Pa were shown in Fig. 1. It indicated that single-layer TaN films is of hexagonal structure at nitrogen partial pressure 0.2– 0.4×10^{-1} Pa and single-layer NbN film is mainly of cubic structure at $P_{N_2} = 0.2 \times 10^{-1}$ Pa, but mainly hexagonal structure at $P_{N_2} = 0.4 \times 10^{-1}$ Pa. The measured lattice constant for TaN is $a = 0.5234$ nm, $c = 0.2975$ nm, $c/a = 0.57$, that for cubic NbN is $a = 0.3036$ nm, and that for hexagonal NbN is $a = 0.3036$ nm, $c = 0.5561$ nm, $c/a = 1.83$.

The X-ray diffraction patterns of NbN/TaN nanomultilayers with modulation period from 2.3 nm to 34.5 nm were shown in Fig. 2. It is clear that NbN/TaN multilayers are hexagonal structure with strong (110) and (300) textures. The peak position of (110) and (300) lattice plane do not move. In comparison of Fig. 2 with Fig. 1c and d, it is found that the crystal structure of NbN/TaN multilayers is the same as that of the single-layer TaN films. The single-layer NbN film is the mixtures of the cubic and hexagonal structure as shown in Fig. 1c and d. But the diffraction lines of NbN did not show in the X-ray diffraction patterns of the composite multilayer films. It is possible that the hexagonal NbN

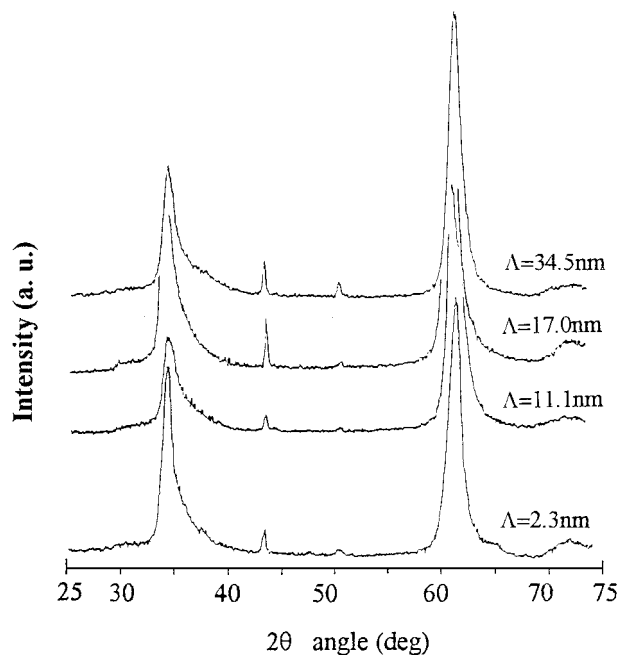


Figure 2 High-angle XRD spectra of NbN/TaN multilayers.

structure is “epitaxially stabilized” by the hexagonal TaN, but it is unlikely because the hexagonal lattice constants of NbN and TaN are so different. Another possibility is that diffraction line of the face cubic or hexagonal structures of NbN layers are overlapped by those of the hexagonal structure of TaN films in the X-ray diffraction patterns. This needs to be verified by other experiments.

3.2. Cross-sectional HREM and electron diffraction

Fig. 3 shows that the electron diffraction patterns of cross-sectional NbN/TaN multilayers with modulation period $\Lambda = 11.1$ nm. It is found that the electron diffraction rings of NbN/TaN multilayers are a combination of the cubic NbN and hexagonal TaN electron diffraction circles. Hence, it can be confirmed that the diffraction peaks of face cubic NbN in XRD spectra were overlapped by that of the hexagonal TaN.

Fig. 4 is HREM photograph of NbN/TaN multilayers that gave the electron diffraction patterns in Fig. 3.

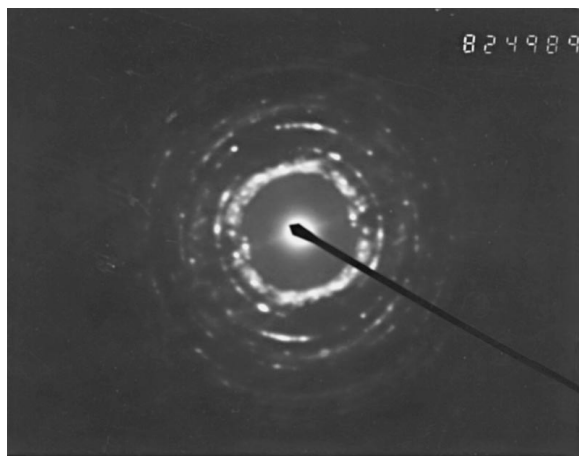


Figure 3 Electron diffraction of cross-sectional specimen.

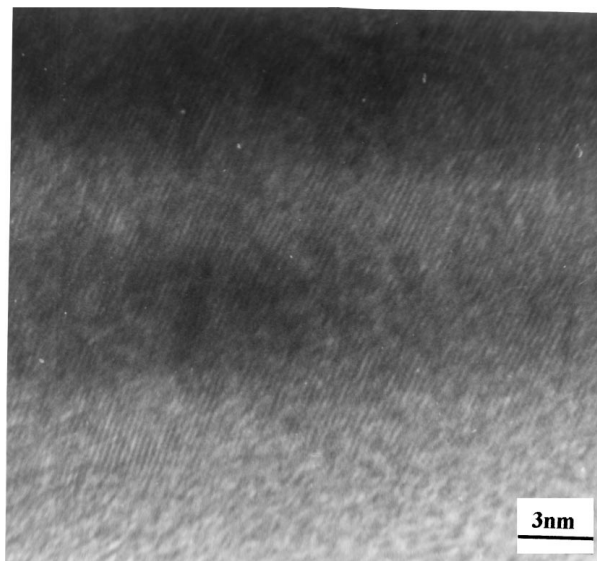


Figure 4 HREM micrograph of NbN/TaN multilayers.

The modulation structure was very sharp and the layers were nearly planar. The TaN layers were dark and NbN layers are bright. In a large grain, the lattice fringes penetrate through interfaces. It means that it takes coherent growth between TaN and NbN. Few dislocations were found in the coherent grains. But lattice fringes distorted at interfaces which indicated that NbN/TaN multilayers still were coherent growth model at $\Lambda = 11.1$ nm. The lattice spacing measured from Fig. 4 is 0.2568 nm. According to the lattice spacing of $d_{(110)} = 0.2617$ nm for the TaN and $d_{(111)} = 0.2535$ nm for NbN, the coherent relationship between (111) of the cubic NbN and (110) of the hexagonal TaN was determined. The lattice mismatch in this case is 3.18%.

3.3. Hardness of NbN/TaN superlattice films

Shown in Fig. 5 is the microhardness of multilayers as a function of the modulation period. The Knoop microhardness values were found to increase rapidly with the increase of the modulation period and reached a maximum of 5100 kgf/mm² at $\Lambda = 2.3$ nm. The hardness kept at high values HK = 4650–5000 kgf/mm² with $\Lambda = 2.3$ –17.0 nm. The hardness decreased rapidly at $\Lambda > 17.0$ nm, and the hardness was 3487 kgf/mm² at

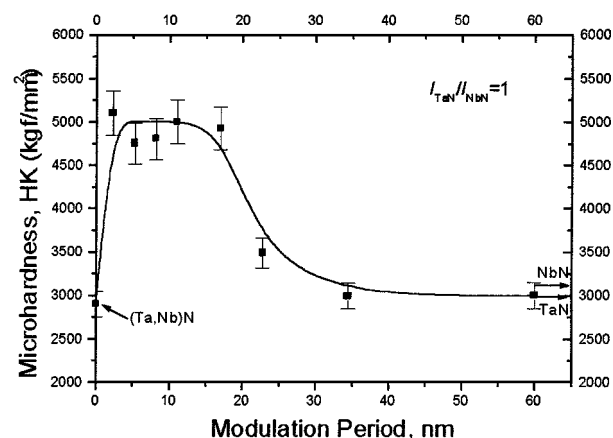


Figure 5 Microhardness of multilayers as a function of the modulation period.

$\Lambda = 22.8$ nm. Further increasing Λ resulted in a relatively slow decrease in hardness and the hardness was 3000 kgf/mm^2 at $\Lambda = 60.0$ nm, which also is comparable with the value calculated from the rule of mixture.

4. Discussion

The results observed from above experiments have shown that there are “superhardness effects” in NbN/TaN multilayers and the hardness anomaly take place at a relatively wide modulation period from 2.3 nm to 17.0 nm.

It is reported that the stable structure of the mono-layer NbN, VN and TaN is all hexagonal [1, 4, 6] on microstructure. But if they have been composed with TiN as multilayers VN/TiN, NbN/TiN and TaN/TiN, the NbN, VN and TaN layers in the films will form metastable face cubic structure which is “epitaxially stabilized” by the cubic TiN. Hence the crystal structure of the NbN/TiN, VN/TiN and TaN/TiN all is epitaxial growth cubic with different lattice mismatch. The superhardness effects were found in these systems. About the anomalous increase of hardness, the coherent strain theory [7, 8] considered that the coherent strain caused by lattice mismatch in epitaxial growth can produce alternating stress fields which inhibit the generation and motion of dislocations, leading to the strength and hardness increase of the films. The maximum hardness occurred at a range of modulation period where coherent stresses exist. The decrease in hardness at smaller modulation period is likely attributable to the interdiffusion or composition intermixing. The decrease at larger modulation period may be the results of the stress relaxation in incoherent interface or the generation and motion of dislocations in the layers with lower elastic modulus. The strain coherent theory has been used to explain the superhardness effects of the NbN/TiN, VN/TiN and TaN/TiN superlattice films in which the hardness peak occurred at 5 nm–9 nm, a short modulation period.

In NbN/TaN multilayers, the NbN layers and TaN layers did not grow epitaxially with the same crystal structure, but with face cubic and hexagonal. Lattice plane match relationship has been discovered between (111) for cubic NbN and (110) for hexagonal TaN. Therefore it may be speculated that even if NbN layers did not take the same crystal structure as TaN layers, the coherent interface with a lattice mismatch 3.18% have led to the alternating stress fields which inhibit the dislocation generation and motion. The interfacial coherent

strain plays a main contribution to the superhardness effects at modulation period smaller than 17.0 nm in NbN/TaN multilayers. In the view of decreasing the free energy of the system, incoherent interface containing dislocation can decrease the free energy of the system. The coherent strain effects disappeared slowly at modulation period larger than 17.0 nm. Therefore, the hardness value decreased slowly. The hardness kept maximum value at a modulation period of 2.3 nm. The phenomenon is considered to result from the interfacial microstructure between NbN and TaN layers. In our experimental condition, there are very few intermixing at interfaces. That is, the interfaces keep a good segregation of the structure and composition at modulation period 2.3 nm. The coherent stresses can still inhibit the motion of the dislocation. Further work needs to be done about this.

5. Conclusion

(1) The NbN layers are cubic crystal structure and TaN layers are hexagonal in the NbN/TaN superlattice films. The lattice plane (111) of NbN is coherent with (110) of TaN and the lattice mismatch is 3.18%.

(2) NbN/TaN superlattice films have superhardness effects. It shows that even if NbN layers did not take the same crystal structure as TaN layers, hardness anomalous phenomenon still can be produced as long as the coherent strains exist.

(3) The superhardness effects of the NbN/TaN multilayers exist at a wide range of modulation period, which is different from the results reported in other systems.

References

1. U. HELMERSSON, S. TODOROVA, S. A. BARNETT, *et al.*, *Journal of Applied Physics* **62**(2) (1987) 481.
2. P. B. MIRKARIMI, L. HULTMAN and S. A. BARNETT, *Appl. Phys. Lett.* **57**(25) (1990) 2654.
3. M. SHINN, L. HULTMAN and S. A. BARNETT, *J. Mater. Res.* **7**(4) (1992) 901.
4. X. CHU, M. S. WONG, W. D. SPROUL, *et al.*, *J. Vac. Sci. Technol.* **A10**(4) (1992) 1604.
5. LI GEYANG, SHI XIAORONG and ZHANG LIUQIANG, *J. of Shanghai Jiao Tong University* **33**(2) (1999) 159.
6. V. H. SOE and R. YAMAMOTO, *Materials Chemistry and Physics* **50** (1997) 176.
7. J. W. CAHN, *Acta Metallurgical* **11** (1963) 1275.
8. M. SHINN, L. HULTMAN and S. A. BARNETT, *J. Mater. Res.* **7**(4) (1992) 901.

Received 3 June 1999

and accepted 3 February 2000